Materials Science and Engineering B 113 (2004) 203–206

www.elsevier.com/locate/mseb

Improvement of kink characteristics performance of GaAs VCSEL with a indium-tin-oxide top transparent overcoating

Fang-I Lai[a], Ya-Hsien Chang[a], T.H. Hsueh[a], H.W. Huang[a], L.H. Laih[a], H.C. Kuo[a,*], S.C. Wang[a], Tai-Cheng Guung[b]

[a] *Institute of Electro-Optical Engineering, National Chiao Tung University, 1001 Ta Hsueh Road, Hsinchu 30056, Taiwan, ROC*

[b] *Institute of Nuclear Energy Research, Taiwan, ROC*

Received 29 March 2004; accepted 29 July 2004

Abstract

We demonstrated the enhancement in the performance of proton-implanted GaAs VCSEL by incorporation of a new p-contact scheme using a Ti and ITO transparent overcoating on the regular p-contact. The kink characteristics in light output power versus current (*L–I*) curve of the VCSEL with the Ti/ITO overcoating were improved with a reduction in the derivative kink factor of as large as 70%. The high-speed response of the overcoated device also shows a more open clear eye and lower jitter of 35 ps operating at 2.125 Gb/s under 10 mA bias and 9 dB extinction ratio compared to the no overcoated device. Better current spreading and uniformity induced by the overcoating could be responsible for these performance improvements.

Keywords: VCSEL; Proton implant; Indium-Tin-Oxide; Kink; High-speed operation

1. Introduction

The vertical cavity surface emitting lasers (VCSELs) have generated research and commercial interests worldwide, because VCSELs possess several unique features over the edge emitting lasers. The VCSELs emit circular beam with low divergence, making optical fiber coupling more efficient and easier than the edge emitting lasers. The VCSELs can be tested on wafer level before packaging, and can be easily fabricated into dense two-dimensional laser arrays. Currently, there are two main categories of VCSELs namely oxide-confined VCSELs and proton-implanted VCSELs. The oxide-confined VCSELs have an oxided boundary surrounding the emitting aperture for index-guiding and current confinement resulting well-defined transverse modes at low bias current [1,2]. However, the oxide VCSELs have a few technical issues. The oxidation procedure depends strongly on materials and processing parameters which could change during the process making control of the aperture size relatively difficult. In addition, the strain and defects introduced by improper oxidation process might have some reliability problems [3]. Compared to the oxide-confined VCSELs, the proton-implanted VCSELs have a relatively simple fabrication process (planar process) and have been demonstrated with good reliability [4]. However, due to the gain-guided nature of the proton implanted VCSELs, the kinks usually occur in light output power versus current (*L–I*) curve [5], and the laser power output jitter and noise also tend to limit the modulated speed around 1.25 Gb/s [4] that hardly meets the 2.125 Gb/s (2x Fiber channel) requirement. In VCSELs, the kinks in *L–I* curve were attributed to change of multi-transverse mode operation [5]. Some reports indicated that the transverse mode structures depend on the driving current [6], and the injection current from the periphery of the top contact aperture into the active region tends to cause current crowding and non-uniform current spreading [7–10].

* Corresponding author. Tel.: +886 3 5712121x31986; fax: +886 3 5716631.
E-mail address: hckuo@faculty.nctu.edu.tw (H.C. Kuo).

0921-5107/$ – see front matter © 2004 Elsevier B.V. All rights reserved.
doi:10.1016/j.mseb.2004.07.091

In the proton-implanted VCSELs, the evolution of transverse mode pattern would be strongly affected by the current crowding and non-uniform current spreading because of the lack of beam confinement by an index-guiding. Additionally, the metal aperture is smaller than the proton-implanted confinement aperture due to the contact concerned. Therefore, the output light which is localized in the periphery of the implant boundary, esulted from the current crowding and non-uniform current spreading would be blocked by the metal contact and occurred at the large kinks in *L–I* curve. Liu et al. also indicated that the non-uniformity and fluctuation in both injected carrier density and junction temperature could affect the frequency of lasing mode [11]. Consequently, the improvement of current spreading and reduction of current crowding in VCSELs could reduce the kinks and thus improve the device modulation speed especially in proton-implanted VCSEL.

Recently, there were reports of using transparent indium-tin-oxide (ITO) replaced regular Ti/Au or Ti/Pt/Au p-contact metal of the VCSELs to increase contact transparency and showed that the ITO has good ohmic contact similar to the regular contact. These include the use of ITO [12,13], Au-plated ITO [14] as the top contact and ITO as top ring contact [15]. However, the effects of these new contact schemes on the VCSEL performances such as kink characteristics of *L–I* curve and modulation response were not clearly mentioned. In this paper, we report results of incorporation of a new p-contact scheme using Ti and ITO transparent overcoating on the regular p-contact of the implanted VCSEL that show substantial improvement in the kink characteristics and the modulation response of the proton-implanted VCSEL.

2. Experiment

The GaAs VCSEL wafer structure was grown on the n^+-GaAs substrate by a metal organic chemical vapor deposition system. The bottom distributed Bragg reflector (DBR) consists of n-type 30.5-period $Al_{0.12}Ga_{0.88}As$/AlAs and the top DBR consists of 19.5-period p-type $Al_{0.12}Ga_{0.88}As$/AlAs. The active region has an undoped three-quantum-well GaAs/$Al_{0.3}Ga_{0.7}As$, a lower linearly-graded undoped-$Al_xGa_{1-x}As$ (x = 0.6 → 0.3) waveguide layer and an upper linearly-graded undoped-$Al_xGa_{1-x}As$ (x = 0.3 → 0.6) waveguide layer. A heavily carbon-doped p-type GaAs cap layer was grown to facilitate p-ohmic contact. Next a regular p-contact metallization of Ti (200 Å)/Au (1500 Å) were deposited by E-beam evaporator with a 15 μm diameter emission aperture and a contact pad size of 350 μm × 350 μm. Then Ge (200 Å)/Au (400 Å)/Ni (140 Å)/Au (1500 Å) layers were deposited as the n-ohmic contact, and annealed in a rapid thermal annealing system (RTA) at 380 °C under N_2 ambient for 30 s. The device was then subjected to the proton implantation with an energy of 200 KeV and a dosage of 1×10^{15} cm^{-2} with an aperture of 20 μm diameter. All the VCSELs were tested prior to the overcoating. The tested

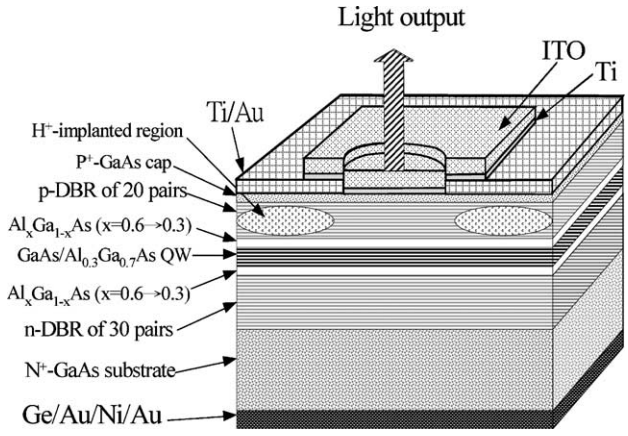

Fig. 1. The schematic of the overcoated VCSEL device.

VCSELs were then overcoated with Ti/ITO transparent film on top of the regular Ti/Au p-contact by RF sputtering in Ar 12 sccm, 5×10^{-3} Torr, at a base pressure of 1.6×10^{-6} Torr and a deposition pressure of 3.3×10^{-4} Torr. The thickness of Ti is 40 Å and ITO (In_2O_3–SnO_2) is 3200 Å. The thin Ti film was chosen because of its high transparency (∼92% at 850 nm), low annealing temperature, good adhesive property and ohmic contact with GaAs. Subsequently, the device was annealed at 380 °C under N_2 ambient for 30 s to form ohmic contact. The dimension of the transparent overcoating is 300 μm × 300 μm slightly smaller than the regular p-contact pad size for easy probing. The schematic of the fabricated VCSEL device is shown in Fig. 1.

3. Results and Discussions

Fig. 2 shows the *L–I–V* characteristics of a typical VCSEL before and after the Ti/ITO overcoating. The maximum light output decreases slightly due to the slightly reduction in transparency from Ti/ITO overcoating. The series resistance of the overcoating VCSEL slightly increases which may be

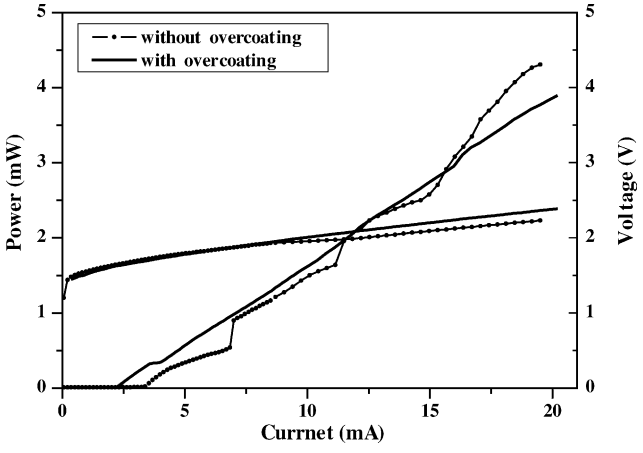

Fig. 2. The *L–I–V* characteristics of a typical VCSEL with and without Ti/ITO transparent overcoating.

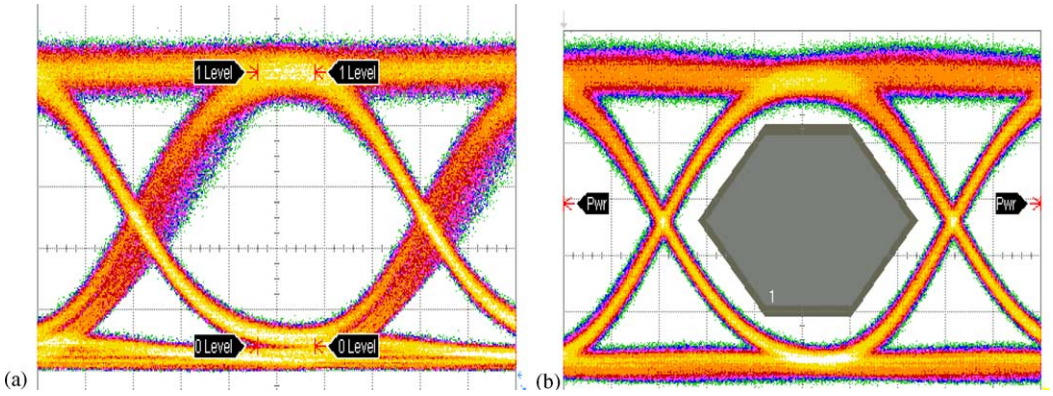

Fig. 3. Eye diagrams of the typical VCSEL device (a) without and (b) with Ti/ITO transparent overcoating operating at 2.125 Gb/s with 10 mA bias and 9 dB extinction ratio. The horizontal scale is 40 ps/div.

due to the additional Ti/ITO annealing process. However, the *L–I* curve of the overcoated VCSEL shows a substantial improvement in the kinks and the improvement of threshold current I_{th} (3.4–2.2 mA) compared with the uncoated VCSEL. It might be due to the improvement of uniform current spreading by the overcoated and the light output would not be deeply affected by the contact metal blocking. The *L–I* curves of the overcoated VCSELs all show a substantial improvement in the kinks compared to the uncoated VCSELs. To quantify the kink characteristics in *L–I* curve, we define a derivative kink factor (DKF) which measure the mean square deviation of the local slope from the average slope, normalized to the average slope of the *L–I* curve as shown below:

$$\text{Derivative kink factor} = \frac{\left((\partial L/\partial I - (\partial L/\partial I))^2\right)^{1/2}}{(\partial L/\partial I)}\Bigg|_{L_{th}}^{L_{max}/2} \quad (1)$$

where L is the light output power, I is the driving current, L_{max} is the maximum light output power, and L_{th} is the light output power at the threshold. To minimize the effect of thermal rollover at higher power output, the DKF is only evaluated from threshold up to $L_{max}/2$. From the *L–I* curves we evaluated DKF value of the VCSEL devices in the same wafer for current range from the threshold to 15 mA, and the DKF values distribute from 0.3 to 1 before the overcoating of Ti/ITO. After overcoating, the DKF values of the VCSELs distribute around 0.2 ± 0.03. This result indicates the DKF values of the VCSELs are more unity and reduced around 33–70% after the Ti/ITO overcoating, clearly indicating the improvement in the kink characteristics and uniformity of the implanted VCSELs after the Ti/ITO overcoating.

To investigate kink-reducing effect on high-speed performance, large signal modulation response was checked. Fig. 3(a) and (b) show the eye diagram of the typical VCSEL device before and after Ti/ITO overcoating, respectively, operating at 2.125 Gb/s with 10 mA bias and 9 dB extinction ratio. The uncoated VCSEL failed to pass the 2.125 Gb/s Eye-Mask and has a large jitter over 40 ps, while the overcoated VCSEL showed a wide open eye pattern and easily passed the 2.125 Gb/s with a jitter of less than 35 ps. The result indicates the Ti/ITO-overcoated VCSEL with lower DKF values has substantially improved in the device high-speed performance characteristic. The improvement in the kink character-

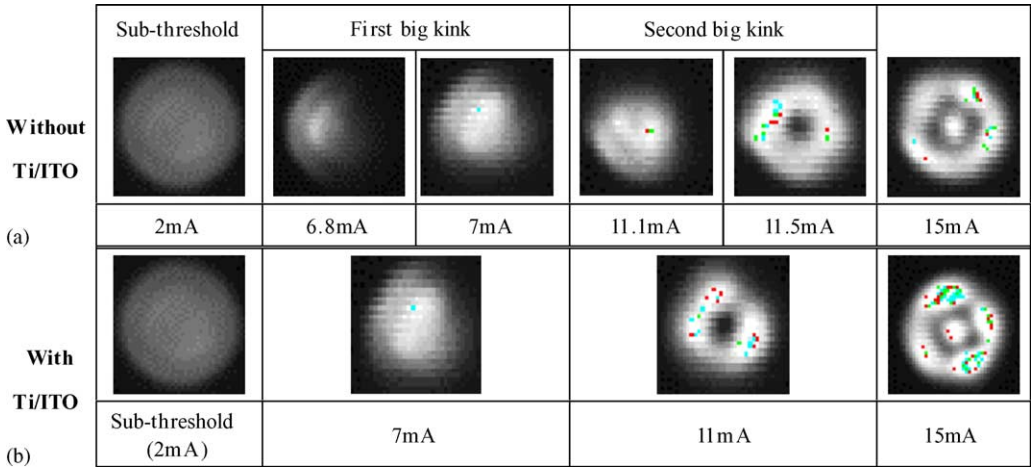

Fig. 4. The near-filed emission patterns of the typical VCSEL device (a) without and (b) with Ti/ITO transparent overcoating at different injecting currents.

istics and the modulation response of the Ti/ITO-overcoated VCSEL maybe the result of better current injection uniformity and carrier spread induced by the overcoating. Since the change of light emission pattern correspond to the change of current injection density [16] into the VCSELs, Fig. 4(a) and (b) compare the near-field optical microscope images of the emission patterns of the VCSEL before and after overcoating in the currents when the kinks occurred. Fig. 4(a) clearly shows the switching between the different lasing mode patterns when large kinks took place in *L–I* curve and the large kinks occurred when the light output might have been partly blocked by metal contact. For comparison, emission patterns of the overcoated VCSEL were shown in Fig. 4, which is more uniform and stable at the same current level. From the near-field images of uncoated and overcoated VCSELs, the overcoating layer did provide better uniformity in the current injection which could lead to the improvement in the kink characteristics in *L–I* curves and high-speed response of the VCSELs.

4. Conclusion

In summary, we demonstrated the enhancement in the performance of proton-implanted VCSEL by using a Ti/ITO overcoating on the regular p-contact. The kink characteristics of the VCSEL with the Ti/ITO overcoating show substantial improvement with as large as 70% reduction in the derivative kink factor. The high-speed response of the overcoated device shows better performance than the uncoated devices with clear eye with 35 ps jitter operating at 2.125 Gb/s with 10 mA bias and 9 dB extinction ratio. These improvements in the implanted VCSEL performance would be due to the better current spreading and uniformity induced by the overcoating. This overcoating technique should be applicable to the other types of VCSELs.

Acknowledgements

This work was supported in part by the National Science Council of Republic of China (ROC) in Taiwan under contract no. NSC91-2215-E009-030 and by the Academic Excellence Program of the ROC Ministry of Education under the contract no. 88-FA06-AB. The authors thank the Institute of Nuclear Energy Research (INER) for proton implantation. They would also like to thank Dr. C. H. Lin of Agilent Techology, Dr. C. P. Kuo and Dr. G. Hasnain of LuxNet corporation, and Dr. C. P. Sung and Dr. H. P. Yang of ITRI for technical discussion.

References

[1] C.W. Wilmsen, H. Temkin, L.A. Coldren (Eds.)„ Cambridge University Press, 1999.
[2] K.L. Lear, A. Mai, K.D. Choquette, S.P. Kilcoyne, R.P. Schneider Jr., K.M. Geib, IEE Electron Lett. 32 (1996) 457.
[3] D.T. Mathes, R. Hull, K. Choquette, K. Geib, A. Allerman, J. Guenter, B. Hawkins, R.A. Hawthorne, in: C. Lei, S.P. Kilcoyne (Eds.), Proceedings of the Vertical-Cavity Surface-Emitting Lasers VII, SPIE 2003, 2003, pp. 67–82.
[4] A. Tatum, A. Clark, J.K. Guenter, R.A. Hawthorne, R.H. Johnson, in: K.D. Choquette, C. Lei (Eds.), Proceedings of the Vertical-Cavity Surface-Emitting Lasers IV, SPIE 2000, 2000, pp. 2–13.
[5] K.D. Choquette, S.P. Kilcoyne, K.L. Lear, R.P. Schneider, IEEE Photonics Technol. Lett. 8 (1996) 740–742.
[6] C.J. Chang-Hasnain, J.P. Harbison, G. Hasnian, A.C. Von Lehmen, L.T. Florez, N.G. Stoffet, IEEE J. Quantum Electron. 27 (1991) 1402–1409.
[7] N.K. Dutta, J. Appl. Phys. (1990) 68.
[8] W. Nakwaski, M. Osinski, IEEE J. Quantum Electron. (1991) 27.
[9] H. Wada, D.I. Babic, M. Ishikawa, J.E. Bowers, Appl. Phys. Lett. 60 (1992) 2974–2976.
[10] S. Sekiguchi, T. Miyamoto, T. Kimura, G. Okazaki, F. Koyama, K. Iga, Jpn. J. Appl. Phys. Part 1 39 (2000) 3997–4001.
[11] Y. Liu, W.C. Ng, B. Klein, K. Hess, IEEE J. Quantum Electron. 39 (2003) 99–108.
[12] M.A. Matin, A.F. Jezierski, S.A. Bashar, D.E. Lacklison, T.M. Benson, T.S. Cheng, J.S. Robers, T.E. Sale, J.W. Orton, C.T. Foxon, A.A. Rezazadeh, IEE Electron. Lett. 30 (1994) 318–320.
[13] C.L. Chua, R.L. Tornton, D.W. Treat, V.K. Yang, C.C. Dunnrowicz, IEEE Photonics Tech. Lett. 9 (1997) 551–553.
[14] R. Thornton, Y. Zou, J. Tramontana, M.H. Crawford, R.P. Schneider, K.D. Choquette, Proceedings of the Conference 1995 IEEE LEOS, San Francisco, CA, 1995, p. 108.
[15] W.-J. Jiang, M.-C. Wu, H.-C. Yu, C.-Y. Huang, C.-P. Sung, J.-Y. Chi, Solid-State Electron. (2002) 46.
[16] L. Roy, IEEE J. Quantum Electron. 15 (1979) 718–726.